A Dual-Mode Narrow-Band Channel Filter and Group-Delay Equalizer for a Ka-Band Satellite Transponder

Sungtek Kahng, Man Seok Uhm, and Seong Pal Lee

This paper presents the design of a narrow-band channel filter and its group-delay equalizer for a Ka-band satellite transponder. We used an 8th order channel filter for high selectivity with an elliptic-integral function response and an inline configuration. We designed a 2-pole, reflection-type, group-delay equalizer to compensate for the steep variation of the group-delay at the output of the channel filter, keeping the thermal stability at ±7 ns of group-delay variation at the band edges over 15–55 °C. We devised a new tuning technique using short-ended dummy cavities and used it for tuning both the filter and equalizer; this removes the necessity of additional tuning after the cavities are assembled. Through measurement, we demonstrate that the group-delay-equalized filter meets the equipment requirements and is appropriate for satellite input multiplexers.

Keywords: Dual-mode, narrow-band filter, group-delay equalizer, Ka-band, satellite.

I. Introduction

Satellites have played outstanding roles in linking remote areas for communication via reception and transmission antennas and passive, active, and power-handling components [1], [2]. In general, a satellite system is given a limited frequency resource, and this has led to designing components based on narrow bands. Channel filters are among the narrow-band designs, and a number of design techniques have been developed and successfully adopted in the input multiplexer.

To provide service with a narrow band and high selectivity, researchers have chosen an elliptic integral function for amplitude approximation. This function accommodates multiple-mode couplings in a filter structure, which can decrease the volume and mass. In line with this, researchers have used and reported on dual-mode waveguide filters [3]-[23].

Frequency-wise, the signal entering the input multiplexer is divided through channel filters of a higher order, each of which has a lower insertion loss in its passband and larger rejection in the other channels. Unfortunately, the group-delay of its output varies abruptly in the passband and results in thermal instability. To circumvent this problem, some researchers have introduced the concept of group-delay equalization with a self-equalized filter and an external group-delay equalizer. The former is a filter with group-delay equalization and has shown thermally stable performance [13]-[15]. However, the design of the self-equalized filter requires very careful steps in determining the number and locations of equalization poles and its tuning is highly complex. On the other hand, an external equalizer is separated from the associated filter and this simplifies the

Manuscript received Aug. 12, 2002; revised June 11, 2003.

Sungtek Kahng (phone:+ 82 42 860 6231, email: s-kahng@etri.re.kr), Man Seok Uhm (email: msuhm@etri.re.kr), and Seong Pal Lee (email: spallee@etri.re.kr) are with Radio & Broadcasting Research Laboratoty, ETRI, Daejeon, Korea.

overall design and tuning process [16]-[18], providing more flexibility with which the amplitude can be equalized along with the group-delay.

In such a design method, all the coupling elements of the network are directly used as optimization variables for minimizing the difference between the group-delay response and the specification mask [16]. This solution often turns out to be non-optimal. On the other hand, Hsu et al. introduced an approximation and synthesis scheme in which the poles and zeros of the impedance function of the structure were found with the evaluation of the group-delay response and used to complete the design [17]. However, to date, no one has reported an equalized channel filter chain for a Ka-band application.

This paper introduces an equalized channel response for a Ka-band application by cascading an inline dual-mode filter with an external equalizer. We satisfy the given requirements by an 8-pole pseudo elliptic function filter in combination with a 2-pole reflection type equalizer. The separate design of these components yields lower order structures that facilitate the design and tuning effort. Both components consist of circular waveguide cavities of a TE_{113} resonance mode, rectangular and cross-shaped irises, and tuning and coupling screws. Prior to designing the equalizer, we computed the coupling elements of the filter. We then obtained the design parameters of the equalizer to minimize the error of the overall group-delay response with regard to the specification. More importantly, we experimentally adjusted and ultimately determined the values during the tuning of the equalizer. Specifically, we implemented equalization to cope with a group-delay variation of less than 7 ns at the band edges over 15–55 °C (the heaters beneath the base plate maintain the temperature range). To achieve thermal stability, we used a space-qualified circulator and an isolator in the path from the filter to the equalizer. For tuning, we adopted a new technique using shortened dummy cavities. The measurement results validate the design method.

II. Design

1. Configuration and Specifications

The channel of the Ka-band input multiplexer is composed of the channel filter and group-delay equalizer. The channel filter is followed by the equalizer, which lowers the group-delay variation (Fig. 1). The signal from the filter enters and leaves the reflection type of equalizer by way of a circulator, which is space-qualified for thermal and mechanical performance. From the input port through the output port, WR42 waveguides are used. Table 1 shows the specifications for the channel of the Ka-band input multiplexer. The center frequency f_0 is 21 GHz and the bandwidth Δf is 100 MHz. The return loss will be at least greater than 13 dB, because the circulator chain of a higher return loss will be adopted for channel branching, if necessary.

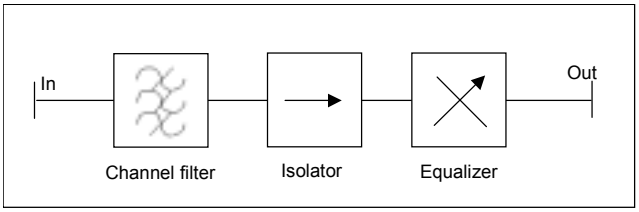

Fig. 1. Channel configuration.

Table 1. Specifications for the channel.

Parameter	Frequency	Spec
Amplitude variation	$f_0 \pm 30$ MHz	0.15 (dBp-p)
	$f_0 \pm 38$ MHz	0.25 (dBp-p)
	$f_0 \pm 45$ MHz	0.50 (dBp-p)
	$f_0 \pm 50$ MHz	1.50 (dBp-p)
Group delay variation	$f_0 \pm 0$ MHz	0.6 (ns)
	$f_0 \pm 20$ MHz	1.8 (ns)
	$f_0 \pm 30$ MHz	2.2 (ns)
	$f_0 \pm 38$ MHz	4.0 (ns)
	$f_0 \pm 45$ MHz	9.5 (ns)
	$f_0 \pm 50$ MHz	22.5 (ns)
Near-band rejection	$f_0 \pm 65$ MHz	–19 (dB)
	$f_0 \pm 80$ MHz	–49 (dB)
	$f_0 \pm 130$ MHz	–55 (dB)
Out-of-band rejection	19–20GHz	<–60 (dB)
Return loss	Within Δf	> 13 (dB)
Insertion loss	Within Δf	< 4 (dB)
Mass		< 600g

2. Channel Filter

We chose a coupling with an 8th order dual-mode elliptic integral function because it best fits the amplitude of the specified frequency response. Similar to those in [3]-[7], the filter transfer function can be expressed as

$$S_{21} = u_0 \frac{S^4 + B_2 S^2 + B_0}{S^8 + A_7 S^7 + A_6 S^6 + A_5 S^5 + A_4 S^4 + A_3 S^3 + A_2 S^2 + A_1 S^1 + A_0}, \quad (1)$$

where $s = \sigma + j\tau$ and $j = \sqrt{-1}$.

Generally, manipulating (1) produces the network parameters of a canonical or folded coupling configuration, and the similarity transforms convert the network to the desired configuration [3]-[7]. Figures 2(a) and 2(b) show the signal flow and channel filter structure resulting from the inline configuration desired in this work. In Fig. 2(a), solid arrows denote sequential couplings, and dotted arrows indicate cross-couplings. The input or output port is coupled through a horizontal slot. The cross-shaped slots are used for intercavity couplings. Especially, with reference to [3]-[7], the 8th order two-port network is mathematically represented as follows:

$$\overline{\overline{Z}} \cdot \bar{I} = \bar{e}, \tag{2}$$

where $\bar{e}^T = (1,0,0,\cdots,0,0)$ is the voltage excitation vector and $\bar{I}^T = (i_1, i_2, i_3, \cdots, i_7, i_8)$ is the current vector including all the resonators. The impedance matrix is expressed by the self- and mutual-coupling values of the network:

$$\overline{\overline{Z}} = j(\tau\,\overline{\overline{U}} + \overline{\overline{M}}) \tag{3}$$

Where $\overline{\overline{U}}$ is the identity matrix and

$$\tau = \frac{f_0}{\Delta f}\left(\frac{f}{f_0} - \frac{f_0}{f}\right). \tag{4}$$

Using the major S-parameters can be represented as

$$S_{21} = -2\sqrt{R_{in}R_{out}}\,i_8 \tag{5}$$

and

$$S_{11} = 1 - 2R_{in}i_1. \tag{6}$$

The normalized input (output) resistance $R_{in}(R_{out})$ is concerned with the input (output) port coupling. The elements of $\overline{\overline{M}}$ or M_{pq} correspond to the intercavity couplings with $M_{pp} = 0$. In addition, M_{pq} can be related to the inverter constant K_{pq} as in [11],

$$K_{pq} = M_{pq}\frac{3\pi \cdot \Delta f}{2f_0}. \tag{7}$$

Once R_{in}, R_{out}, and $\overline{\overline{M}}$ are obtained from (1) using the methods in [3]-[5], rotating $\overline{\overline{M}}$ is repeated until it reaches the desired coupling configuration [6]-[7]. The final M_{pq} will be converted to the initial physical sizes of the slots.

For the waveguides we use, the radius of the circular waveguide and its resonance mode are R_C and TE_{11S}, respectively, with a WR42 (inner size $= a \times b$) input/output port. For convenience, the slot thickness and width are common to all the irises.

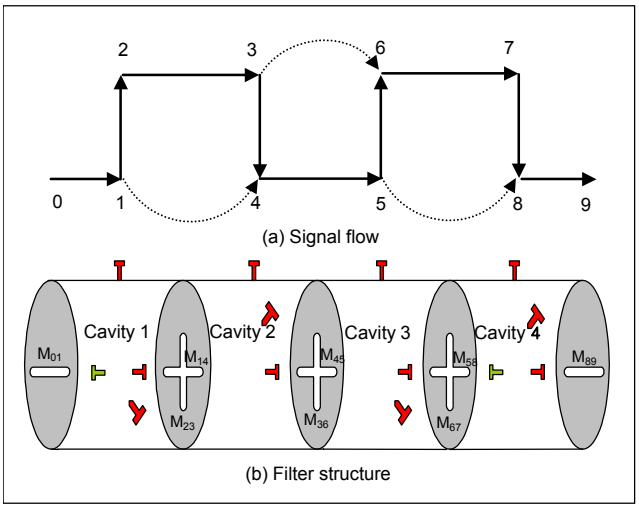

Fig. 2. Signal flow and filter structure.

In determining the initial sizes of the slots for the input (output) port and cavity 1 (cavity 4) and the intercavity coupling, we can use the scattering parameters, reactances, magnetic polarizabilities, etc. In particular, we use the magnetic polarizabilities as goal values for determining the initial sizes. The approximate formula for the input (output) magnetic polarizability $P_{M,io}$ [20] related to external Q is

$$P_{M,io} = \sqrt{\frac{abl_c^3\lambda_{gr}(3R_c^2)R_{in}}{4\pi\lambda_0^2 s^2}}, \tag{8}$$

where λ_0 is the free space wavelength at f_0, λ_{gr} is that of the WR42, and λ_{gc} is that of the circular waveguide. In mode TE_{11S}, cavity length l_c is preliminarily given as $s\frac{\lambda_{gc}}{2}$.

The intercavity coupling magnetic polarizability $P_{M,\mathrm{int},pq}$ is expressed as

$$P_{M,\mathrm{int},pq} = \frac{l_c^3(3R_c{}^2)}{\lambda_0^2}\frac{\Delta f}{f_0}M_{pq}. \tag{9}$$

Now, $P_{M,io}$ and $P_{M,\mathrm{int},pq}$ are equated to the counterpart of the full-wave analysis methods [9]-[11], [18]-[23] or the approximate formula for $P_M{}'$ (infinitesimal thickness) and P_M (slot thickness) as described by

$$P_M = \frac{P_M{}'}{1-\left(\frac{\lambda_l}{\lambda_0}\right)^2}10^{-\left(\frac{2.73t_sA}{\lambda_l}\right)\sqrt{1-\left(\frac{\lambda_l}{\lambda_0}\right)^2}}, \tag{10}$$

where

$$P_M' = \frac{L_S^{\,3}\left[0.187 + 0.052\left(\frac{W_S}{L_S}\right)\left(1-\frac{W_S}{L_S}\right)\right]}{\ln\left(1+2.12\frac{L_S}{W_S}\right)} \tag{11}$$

and L_S, W_S, t_S and λ_l denote the slot length, width, thickness, and slot resonance wavelength, respectively. Constant A takes 3. So far, we have dealt with how to determine the initial sizes.

Next, the initial sizes or the coupling values of the initial sizes need to be verified through measurement, such as monitoring the network analyzer. A number of measurement approaches to this have been introduced, but here we use the scheme in [8], [16], which has a short-ended 1-port configuration. For the input port coupling, after cavity 1 is tuned to f_0, the frequency span from –90° to +90° in the phase-axis is measured and denoted as $\Delta f_{\pm 90^\circ}$ This will be compared to the computed value R_{in} by way of

$$\Delta f_{\pm 90^\circ} = R_{in} \cdot \Delta f. \tag{12}$$

Different from the input port coupling, measurement of the intercavity coupling requires cavities 1 and 2. Cavity 2 is short-ended. The two cavities are synchronously tuned to f_0, and the length of the frequency points for –180° and +180° of the phase is taken as $\Delta f_{\pm 180^\circ,\, pq}$. This is expressed with M_{pq} as in

$$\Delta f_{\pm 180^\circ,\, pq} = M_{pq} \cdot \Delta f. \tag{13}$$

After we determine the slot sizes, we can compute the cavity lengths. The electrical length of a cavity tends to increase by $\frac{\phi_{pq}}{2}$ when coupling occurs through a slot. Therefore, the real cavity should be shortened by the same amount. We used a well-known formula

$$\phi_{pq} = \frac{\lambda_{gc}}{2\pi}\tan^{-1}\left(\frac{2X_{pq}}{Z_0}\right), \tag{14}$$

where the normalized reactance is $\frac{X_{pq}}{Z_0} = \frac{4\pi P_{M,\mathrm{int},pq}}{3R_c^2\lambda_{gc}}$ and Z_0 is the impedance of the waveguide.

Finally, we adjust the screws by following a new tuning technique adopting so-called dummy cavities [25]. Separately tuning the cavities and combining them one by one through the coupling slot perturbs their already-tuned frequencies and necessitates readjustment of the screws. Using dummy cavities for slot coupling before assembling the cavities and adjusting the screws makes additional adjustment later unnecessary. We check the computed and measured reflection coefficients of the real and dummy cavities with the short-end during the tuning.

3. Group-Delay Equalizer

In the reflection-type of group-delay equalizer, the input signal is reflected from the shortened end. Figure 3 shows one such cavity with 2 poles.

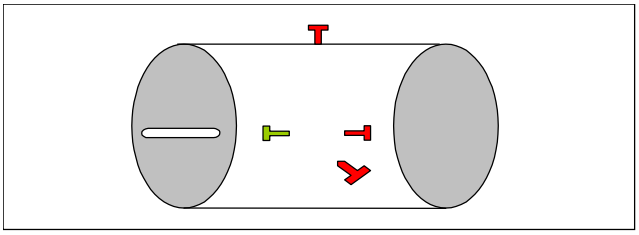

Fig. 3. Group-delay equalizer.

For convenience of design, we decided to have the same radius and resonance mode as the channel filter. The design of the equalizer starts with computing the unknown parameters R_{eq} (normalized input resistance) and K_{12} or M_{12} for the one cavity structure. Because its frequency response is not represented as an elliptic-integral or Chebyscheff function, the following equation's impedance function is alternatively used for our design [8]:

$$Z_{11} = j\frac{\upsilon^2 - M_{12}^2}{\upsilon}, \tag{15}$$

where $\upsilon = \frac{1}{\Delta f}\left(\frac{f}{f_0} - \frac{f_0}{f}\right)$ and Z_{11} is the input impedance of the one-port circuit. S_{11} or reflection coefficient Γ becomes

$$\Gamma = \frac{Z_{11} - R_{eq}}{Z_{11} + R_{eq}}. \tag{16}$$

Hence, the group-delay of the equalizer is expressed as

$$\zeta = -\frac{1}{2\pi}\frac{d}{df}(Phase(\Gamma)). \tag{17}$$

With the parameters of the filter determined beforehand, we varied the unknowns during the simulation to reach the minimum difference between the overall group-delay response and the requirement. The difference corresponds to the error function of the optimization as in [14], [16].

We followed procedures for finding and measuring the initial slot sizes and the cavity length similar to the way we designed

the input (output) port coupling and cavity 1 (cavity 4). In addition, we used a new tuning method.

III. Realization and Test Results

With regard to the specifications shown in Table 1, τ=±1.4 and τ=±1.66 turn out appropriate transmission zeros and (1) can be identified with u_0 = –j0.04, B_2 = 4.72, B_0 = 5.40, and Table 2. The required values M_{pq} and R_{in} (R_{out}) are also obtained as indicated in Table 3. In the symmetric filter structure, $R_{in} = R_{out} = 1.1$, $M_{12} = M_{78}$, $M_{23} = M_{67}$, $M_{34} = M_{56}$, and $M_{14} = M_{58}$. These are listed in Table 2. The external Q is 170.

Table 2. Coefficients of the denominator of the transfer function.

A_7	A_6	A_5	A_4	A_3	A_2	A_1	A_0
2.08	4.72	5.80	6.46	4.82	2.91	1.11	0.24

Table 3. Coupling coefficients for the filter.

Sequential coupling		Cross coupling	
$M_{12}(=M_{78})$	0.903		
$M_{23}(=M_{67})$	0.737	$M_{14}(=M_{58})$	−0.196
$M_{34}(=M_{56})$	0.523		
M_{45}	0.549	M_{36}	−0.00543

When we used the coupling coefficients for finding the slot sizes, we chose 0.7 mm for W_S and 0.4 mm for t_s. Only slot lengths can be obtained with (8) and (11). When $P_{M,io}$ and $P_{M,\text{int},pq}$ are 26.5 and 6.8, the slot lengths become around 5.9 mm and 4.7 mm (Fig. 4). These are converted to $\Delta f_{\pm 90^\circ} = 123\text{MHz}$ and $\Delta f_{\pm 180^\circ,pq} = 75\text{MHz}$ and are verified in Figs. 5(a) and 5(b). Subsequently, we computed the cavity lengths. We used irises, cavities, and screws manufactured by Invar 36 to maintain frequency stability of the responses, i.e., to satisfy all specifications over an operating temperature range of ± 20 °C. The measured rejection response of the sole filter, obtained after manufacturing and tuning, is shown in Fig. 6 in combination with the synthesized characteristic and the specification. The realized (equiripple) bandwidth was 102 MHz, while the rejection at 65 MHz below and above the center frequency was approximately 31 dB. Thus, the design provides a margin of 11 dB implying compliance of the rejection requirement over the operating temperature range.

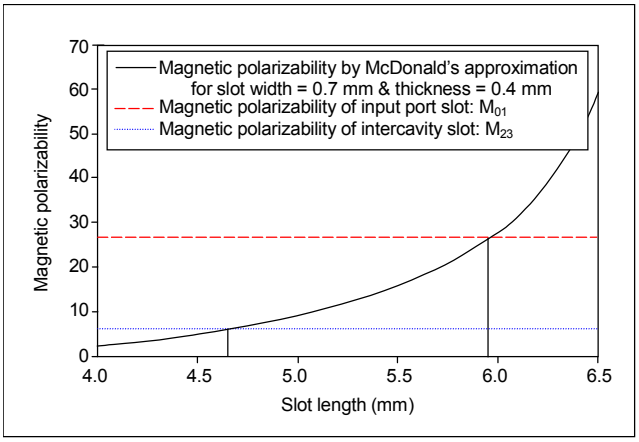

Fig. 4. Initial slot sizes vs. magnetic polarizabilities.

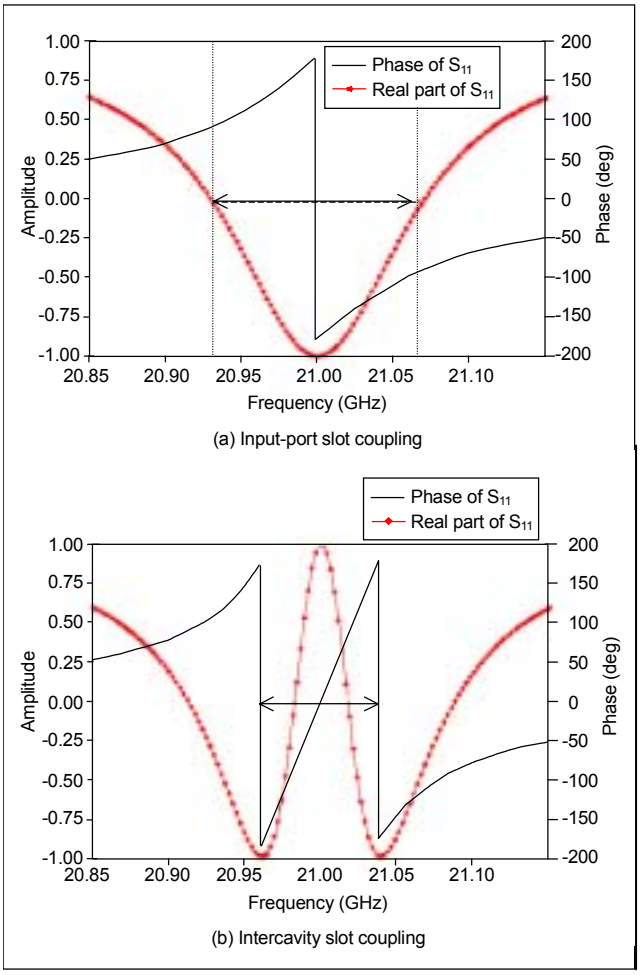

Fig. 5. Measurement of the slot coupling.

The filter exhibits an insertion loss of 0.97 dB at the center frequency and the passband return loss meets the requirement of 13 dB (Fig. 7). Apart from the concept of the magnitude, Fig. 8 shows the variation of group-delay and amplitude. It is clear that the amplitude and group-delay vary more than their specified

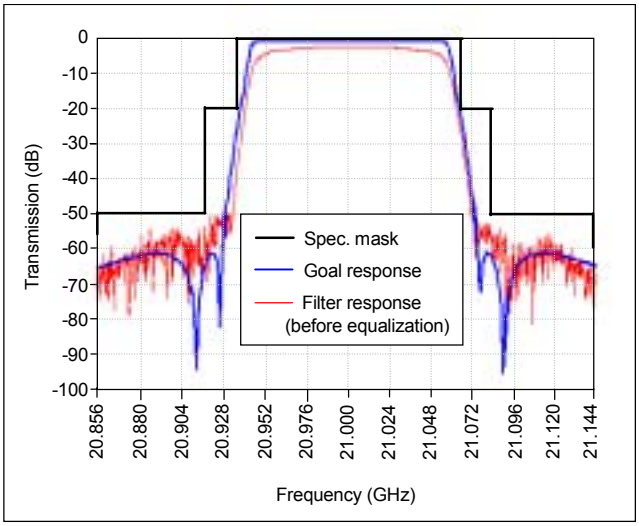

Fig. 6. Transmission of the filter before equalization: goal (blue line), measurement (red line), specification mask (black line).

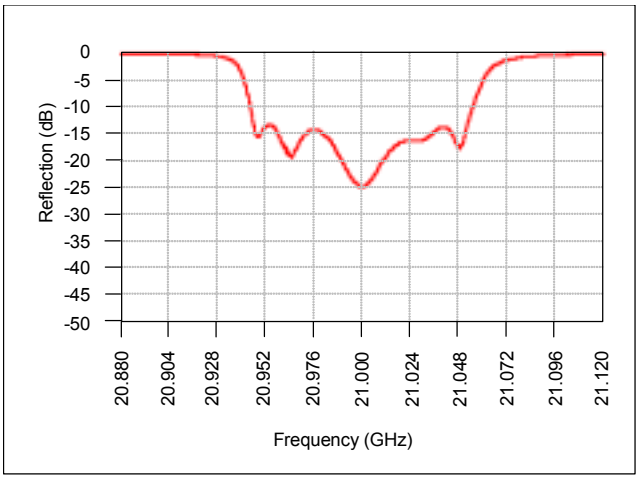

Fig. 7. Reflection of the filter before equalization.

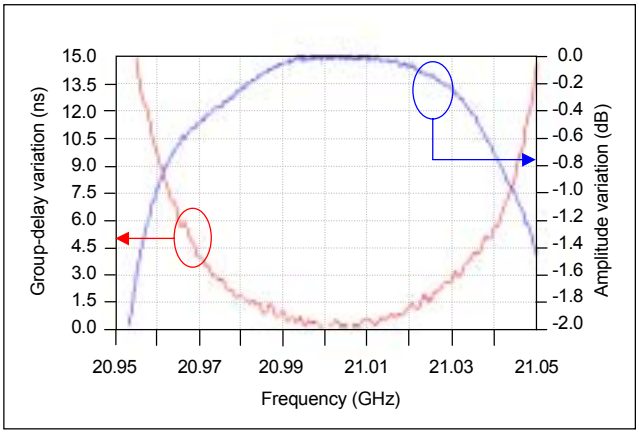

Fig. 8. Passband variation of the amplitude and group-delay before equalization for the ambient temperature.

levels at the output of the filter. This necessitates a group-delay equalizer, which compensates for the amplitude as well as for group-delay variation.

The unknowns for the group-delay equalizer are computed as $R_{eq} = 1.005$ and $K_{12} = 0.0146$ through the 2-variable Secant-concept of error minimization with the previously simulated response of the filter. Figure 9 provides the simulated results of the group-delay both before and after equalization. The two values are converted to the physical sizes of the equalizer that is manufactured with its W_S and t_S the same as those of the filter. As with the filter, the irises, cavities, and screws are manufactured by Invar 36, when there is a thermal shift of about ± 0.8MHz over ∓ 10°C. Figure 10 shows the magnitudes of S_{21} and S_{11} after equalization with the specification mask. These are measured at an ambient temperature. The bandwidth did not change, an insertion loss

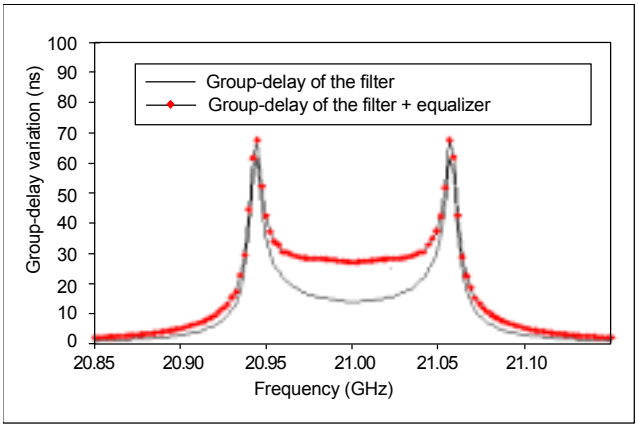

Fig. 9. Comparing the group-delay before and after equalization.

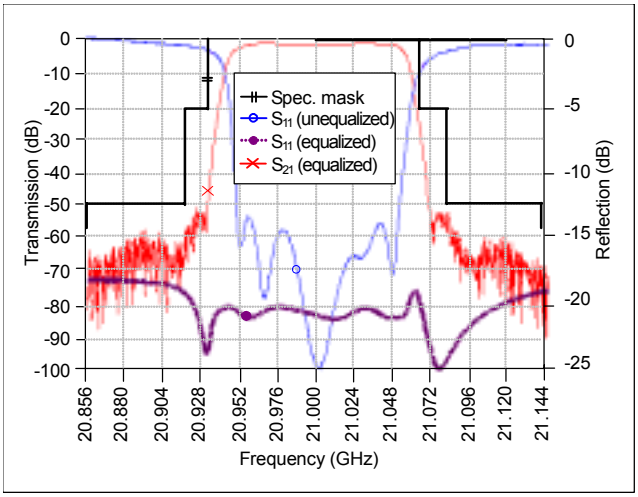

Fig. 10. Transmission (red line) and reflection (purple dotted line) of the filter after equalization for the ambient temperature, with a specification mask (black line) and reflection (blue line) of the unequalized case.

of 3.10 dB at f_0 was less than 4 dB, and the return loss performed well. The rejection still had a margin over 11 dB and did not cause any serious thermal degradation.

Next, we had to verify how the equalization was carried out. The variation measurements were obtained at an ambient temperature, 15°C and 55°C (Fig. 11). Across the three temperatures, the amplitude and group-delay were much flattened in the passband, and the amplitude in each case varied above the specification mask seen in Fig. 11. Especially, the equalized group-delay showed thermal stability over the changed temperature with a variation of less than 7 ns at the band edges over 15°C–55°C. This resulted from the good equalization and is appropriate for use in a satellite system.

In Fig. 12, a spurious response of the channel is given with a mask ranging from 19 GHz through 20 GHz. For the out-of-band rejection, S_{21} is less than –60 dB and complies with the requirement. The two peaks around 22.35 GHz are quite distant from the band and can be suppressed by a simple lowpass filter if necessary. Finally, Fig. 13 is a photograph of the group-delay equalized filter. With its brackets included, its total mass is only 578 g.

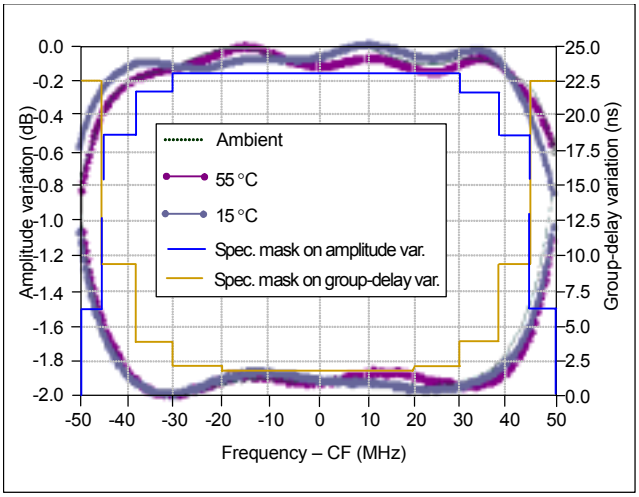

Fig. 11. Passband variation of the amplitude and group-delay after equalization for the ambient temperature (dotted line), 15 °C (gray line with circles), and 55 °C (purple line with diamonds). CF = Center Frequency.

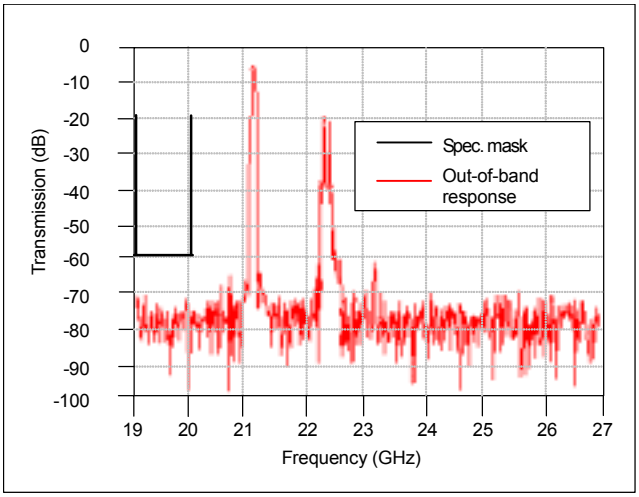

Fig. 12. Out-of-band response (red line) of the channel with a specification mask (black line).

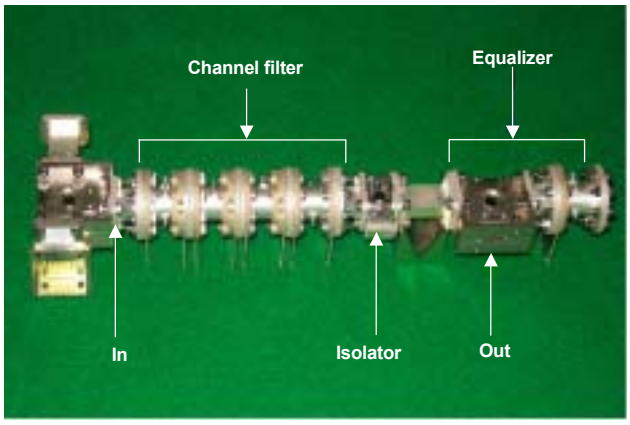

Fig. 13. Photograph of the group-delay equalized filter.

IV. Conclusion

This paper presented an 8th-order narrow-band channel filter and its 2-pole group-delay equalizer, which we designed, manufactured, and efficiently tuned by a new tuning technique for a Ka-band input multiplexer for a satellite transponder. Our measurements revealed that the channel filter has good rejection with the desired bandwidth, but has poor performance of amplitude and group-delay variation. However, the group-delay equalizer much improved the performance, and the entire channel results complied with the specific requirements. Thus, our group-delay equalized channel filter is shown to be suitable for the satellite input multiplexer.

References

[1] K. Lim et al, "A Satellite Radio Interface for IMT-2000," *ETRI J.*, vol. 24, no. 6, Dec. 2002, pp. 415-428.

[2] M.-Q. Lee et al, "Phase Noise Reduction of Microwave HEMT Oscillators Using a Dielectric Resonator Coupled by a High Impedance Inverter," *ETRI J.*, vol. 23, no. 4, Dec. 2001, pp. 199-201.

[3] A.E. Williams, "A Four-Cavity Elliptic Waveguide Filter," *IEEE Trans. on Microwave Theory and Technique*, vol. 18, no. 12, Dec. 1970, pp. 1109-1114.

[4] A.E. Atia and A.E. Williams, "New Types of Waveguide Bandpass Filters," *COMSAT Technical Review*, vol. 1, no. 1, 1971, pp. 21-43.

[5] A.E. Atia and A.E. Williams, "Narrow-Bandpass Waveguide Filters," *IEEE Trans. on Microwave Theory and Technique*, vol. 20, no. 4, Apr. 1972, pp. 258-265.
[6] R.J. Cameron and J.D. Rhodes, "Asymmetric Realizations for Dual-Mode Bandpass Filters," *IEEE Trans. on Microwave Theory and Technique*, vol. 29, no. 4, Jan. 1981, pp. 51-58.
[7] R.J. Cameron, "A Novel Realization for Microwave Bandpass Filters," *ESA J.*, vol. 3, 1979, pp. 281-287.
[8] A.E. Atia and A.E. Williams, "Measurements of Intercavity Couplings," *IEEE Trans. on Microwave Theory and Technique*, vol. 23, no. 6, June 1975, pp. 519-522.
[9] K.-L. Wu, "An Optimal Circular-Waveguide Dual-Mode Filter without Tuning Screws," *IEEE Trans. on Microwave Theory and Technique*, vol. 47, no. 3, Mar. 1999, pp. 271-276.
[10] L. Accatino et al, "A Four-Pole Dual-Mode Elliptic Filter Realized in Circular Cavity without Screws," *IEEE Trans. on Microwave Theory and Technique*, vol. 44, no. 12, Dec. 1996, pp. 2680-2687.
[11] Ji-Fuh Liang et al, "Dual-Mode Dielectric or Air-Filled Rectangular Waveguide Filters," *IEEE Trans. on Microwave Theory and Technique*, vol. 42, no. 7, July 1994, pp. 1330-1336.
[12] T.A. Abele et al, "An Adjustable Narrow Band Microwave Delay Equalizer," *IEEE Trans. on Microwave Theory and Technique*, vol. 15, no.10, Oct. 1967, pp. 566-574.
[13] H. Gregg et al, "A New Generation of 12GHz Channel Demultiplexer For Communications Satellite Applications," *European Microwave Conference,* vol. 87, no. 1, Sept. 1987, pp. 707-712.
[14] C.M. Kudsia, "Synthesis of Optimum Reflection Type Microwave Equalizers," *RCA Review*, vol. 31, Sept. 1970, pp. 571-595.
[15] C.M. Kudsia et al, "Linear Phase Versus Externally Longitudinal Dual-Mode Filters for Space Applications," *IEEE MTT-S Int'l Microwave Symp. Dig.,* vol. 78, no. 1, 1978, pp. 220-222.
[16] M.H. Chen, "The Design of a Multiple Cavity Equalizer," *IEEE Trans. on Microwave Theory and Technique*, vol. 30, no. 9, Sept. 1982, pp. 1380-1383.
[17] H.-T. Hsu et al, "Design of Coupled Resonators Group Delay Equalizers," *IEEE MTT-S Int'l Microwave Symp. Dig.,* vol. 2001, no. 1, May 2001, pp. 1603-1606.
[18] R. Keller et al, "Fast and Rigorous CAD of Phase Delay Equalizers by Mode Matching Techniques Including Losses," *IEEE MTT-S Int'l Microwave Symp. Dig.,* vol. 2001, no. 1, May 2001, pp. 921-924.
[19] S. Kahng et al, "An Efficient Impedance Matrix Calculation Using the SDDI Technique," *ETRI J.*, vol. 23, no. 2, June 2001, pp. 71-76.
[20] J. Bornemann et al, *Waveguide Components for Antenna Feed Systems. Theory and CAD*, Norwood, MA: Artech House, 1993.
[21] R. Vahldieck et al, "Mode-Matching Analysis of Circular-Ridged Waveguide Discontinuities," *IEEE Trans. on Microwave Theory and Technique*, vol. 46, no.2, Feb. 1998, pp. 191-195.
[22] S. Amari, J. Bornemann, and R. Vahldieck, "Fast and Accurate Analysis of Waveguide Filters by the Coupled-Integral-Equations Technique," *IEEE Trans. on Microwave Theory and Technique*, vol. 45, no. 9, Sept. 1997, pp. 1611-1618.
[23] F. Alessandri et al, "A Full-Wave CAD Tool for Waveguide Components Using a High-Speed Direct Optimizer," *IEEE Trans. on Microwave Theory and Technique*, vol. 43, no. 9, Sept. 1995, pp. 2046-2052.
[24] N. McDonald, "Simple Approximation for the Longitudinal Magnetic Polarizabilities of Some Small Apertures," *IEEE Trans. on Microwave Theory and Technique*, vol. 36, no. 7, July 1988, pp. 1141-1144.
[25] J. Lee and S. Kahng et al "A Tuning Method Using a Dummy cavity for Dual-Mode Cavity Filters," *Proc. IEEE Radio and Wireless Conf.*, Boston, Aug.12-16, 2002, pp. 67-70.

Sungtek Kahng was with Hanyang University in Seoul, Korea, and received the PhD degree in electronics and communication engineering in 2000, with a specialty in radio science and technology. From 1996 through 2000, he held the positions of Primary Research Assistant and Researcher at the Institute of Science and Technology of the same university, where he mainly conducted research on computational electromagnetics and its development and applications. Since 2000, he has been working for the Electronics and Telecommunications Research Institute in Daejeon, Korea, as a Senior Staff of Research and Development. He has been involved in research, design and development of microwave equipment and systems for satellites and has much interest in numerical modeling, analysis, electromagnetic characterization of RF devices, and circuits.

Man Seok Uhm received the BS and MS degrees in electronic engineering from Chungang University in Korea, in 1987 and 1989. He joined the Electronics and Telecommunications Research Institute in Daejeon, Korea in 1982, as a Senior Staff of Research and Development.

Seong Pal Lee received the BS degree in electrical engineering from Seoul National University in 1987 and MS and PhD degrees in electrical and computer engineering from the Polytechnic Institute of New York (formerly, PIB) in 1986 and 1990. Since 1980, he has been with the Electronics and Telecommunications Research Institute in Daejeon, Korea, as a Principal Staff of Research and Development, and Project Manager of the Communication Satellite Development Center.